arXiv:1310.8251v1 [astro-ph.CO] 30 Oct 2013

Constraints on Holographic cosmologies from strong lensing systems

Víctor H. Cárdenas,* Alexander Bonilla,† and Verónica Motta‡

Departamento de Física y Astronomía,

Facultad de Ciencias, Universidad de Valparaíso,

Gran Bretaña 1111, Valparaíso, Chile

Sergio del Campo§

Instituto de Física, Pontificia Universidad Católica de Valparaíso,

Av. Brasil 2950, Valparaíso, Chile.

(Dated: January 16, 2022)

Abstract

We use strongly gravitationally lensed (SGL) systems to put additional constraints on a set of holographic dark energy models. Data available in the literature (redshift and velocity dispersion) is used to obtain the Einstein radius and compare it with model predictions. We found that the ΛCDM is the best fit to the data. Although a preliminary statistical analysis seems to indicate that two of the holographic models studied show interesting agreement with observations, a stringent test lead us to the result that neither of the holographic models are competitive with the ΛCDM. These results highlight the importance of Strong Lensing measurements to provide additional observational constraints to alternative cosmological models, which are necessary to shed some light into the dark universe.

PACS numbers: 95.30.Sf, 98.62.Sb, 98.80.-k

*Electronic address: victor.cardenas@uv.cl

†Electronic address: alex.bonilla@uv.cl

‡Electronic address: veronica.motta@uv.cl

§Electronic address: sdelcamp@ucv.cl

I. INTRODUCTION

The accelerating expansion of the Universe is a fundamental challenge to both particle physics and cosmology. Although initially the evidence emerge from studies of Type Ia supernova (SNIa) [1], now we have strong indications from probes like the large scale structure (LSS, [2]), cosmic microwave background (CMB, [3]), the integrated Sachs–Wolfe effect (ISW, [4]), baryonic acoustic oscillations (BAO, [5]) and gravitational lensing [6]. The source of this mysterious cosmic acceleration is dubbed dark energy (DE). The simplest candidate is a cosmological constant Λ, which leads to the successful Λ-cold-dark-matter (ΛCDM) model. Although it fits most of the observational data rather well, it suffers from two main problems, namely: the low value of the vacuum energy and the coincidence problem [7]. To address these two problems, the cosmological constant is replaced by a time varying quantity, leading to the dynamical DE models. The most studied models are scalar field ones which comprehend, e.g., quintessence [8], K-essence [9] and tachyon fields [10]. Usually, dark matter (DM) and DE are assumed to evolve independently, however, there is no reason to neglect interactions in the dark sector [11]. Because both dark components are characterized through their gravitational effects, it is natural to consider unified models of the cosmological substratum in which one single component plays the role of DM and DE simultaneously. Examples of this type of models are the Chaplygin gas [12], and bulk-viscous models [13].

Among the many approaches to describe the dark components, the holographic DE models have received considerable attention [14, 15]. The holographic dark energy is one of the emergent dynamical DE model proposed in the context of fundamental principle of quantum gravity, so called holographic principle. This principle arose from black hole and string theories. The holographic principle states the number of degrees of freedom of a physical system, apart from being constrained by an infrared cutoff, it should be finite and it should scale with its bounding area rather than with its volume[16]. Specifically, it is derived with the help of entropy-area relation of thermodynamics of black hole horizons in general relativity which is also known as the Bekenstein-Hawking entropy bound, i.e., $S \simeq M_p^2 L^2$, where S is the maximum entropy of the system of length L and $M_p = 1/\sqrt{8\pi\, G}$ is the reduced Planck mass. In general terms, the inclusion of the holographic principle into cosmology, makes possible to find the upper bound of the entropy contained in the universe[17].

Using this idea it was possible to obtain a theoretical relation between a short distance (ultraviolet) cutoff and a long distance (infrared, IR) cutoff [15]. Considering L as a cosmological length scale, different choices of this cutoff scale results in different DE models. For example, when identifying L with the Hubble radius H^{-1}, the resulting DE density turns out to be very close to the observed critical energy density [15]. Li [18] studied the use of both the particle and event horizons as the IR cutoff length. He found that apparently only a future event horizon cutoff can give a viable DE model. More recently, it was proposed a new cutoff scale, given by the Ricci scalar curvature [19, 20], resulting in the so-called holographic Ricci DE models. Thus, in general terms, the holographic DE model suffers the IR-cutoff choice problem. On the other hand, holographic DE model have been tested and constrained by various astronomical observations [21], in some cases also including spatial curvature [22]. A special class are those models in which the holographic DE is allowed to interact with DM[23–26].

In this article we use strongly gravitationally lensed (SGL) systems, to provide additional constraints on these holographic DE models. The idea of using such systems was discussed first in [27] and also in [28]. We use the data set first used in [29] (see also [30]) consisting in 70 data points from Sloan Lens ACS (SLACS), and galaxy clusters from optical and X-ray surveys [53, 54].

Some of the holographic DE models we chose corresponds to those first discussed in [31] under the constraint of various astronomical observations, such that SNIa and from the history of the Hubble parameter. Using SGL features we compared three cases of interacting DE models, and studied the relation between the energy density ratio of DM and DE and the equation-of-state (EoS) parameter in these cases. An interesting result of this study is that the role of potential interactions in the dark sector could be clarified. It is noteworthy that any interaction model introduces relations between the matter content and the EoS.

This paper is organized as follows: In Section II we describe the data considered in this work to put in tension our theoretical models. The latter are described in section III, the results are displayed in section IV, and the conclusions in section V.

II. THE SAMPLE

The discovery of the first lensed quasar Q0957+561[32] brings an interesting possibility to use SGL systems as cosmological tools [55, 56]. Some of the statistical methods which use strong lensing to constraint cosmological models are for example: (i) The probability of strong lensing event is known to be sensitive to dark energy [57],[58]. Recent results are in agreement with LCDM cosmological model e.g., [59], [60], [61]. (ii) The differential probability distribution of lens redshifts is fairly insensitive to both the source quasar population and magnification bias [62], [63], [64], [65], [66], [67]. Unfortunately, small number statistics remain a significant limitation for the cosmological results.

Lensing phenomena are sensitive to the geometry of the cosmological background since the appearance of an image depends on the distances between source, lens and observer [33]. By having information about these distances from observations (using redshift measurements) we will be able to constrain cosmological models.

The advantage of this method is that it is independent of the Hubble constant value and is not affected by dust absorption or source evolutions (e.g., as SNIa [68]). However, it depends on the measurements of σ and lens modeling (e.g. singular isothermal sphere (SIS) or singular isothermal ellipsoid (SIE) assumption).

Hundreds of lens systems are being discovered in ongoing surveys (Herschel Lensing Survey, [69], South pole telescope, [70]) and in the next decade 10000 systems are expected to be detected with the Large Synoptic Survey Telescope and Euclid [71]. With such a huge number of data, and larger redshift coverage, SGL will provide a level of precision in cosmology higher than other technics.

In what concern to data manipulation, and following [29], we selected 59 strong lens systems from the Sloan Lens ACS Survey (SLACS, [51]) and the Lens Structure and Dynamic survey (LSD, [43, 44]), and 11 from CfA-Arizona Space Telescope LEns Survey [72]. SLACS systems where selected from the Sloan Digital Sky Survey (SDSS) based on the presence of absorption-dominated galaxy continuum at one redshift and emission lines at another higher redshift ([50]). CASTLES obtained HST images for known galaxy-mass gravitational lens systems.

It has been shown the singular isothermal sphere (SIS) is an accurate first-order approximation for an elliptical galaxy acting as lens ([45–48, 73–76]). In these cases, the modeled

SIS velocity dispersion (σ_{mod}) is in good agreement with the central velocity dispersion measured spectroscopically (σ_{obs})([46–49]). The Einstein ring radius is defined as

$$\theta_E = 4\pi \frac{D_A(z_L, z_S)}{D_A(0, z_S)} \frac{\sigma^2}{\overline{c}^2} \tag{1}$$

where $\overline{c}$ represents the speed of light and σ refers to the central velocity dispersion observed (σ_{obs}) or modeled (σ_{mod}).

Based on observations of X-ray, there is a strong indication that DM halos are dynamically hotter than the luminous stars, then the velocity dispersion σ_{SIS} of the SIS model is different from the observed stellar velocity dispersion σ_{obs} [77]. The authors of [29] and [78] have used a SIS model and an extra factor f_E to account for: (i) systematical errors in the observed velocity dispersion, (ii) differences between θ_E obtained from SIS and SIE and image separation.

However, [47] has used the SLACS lenses to compare the central velocity dispersions with the best SIE lensing model. They found a factor $f = \sigma_0/\sigma_{SIE} = 1.01 \pm 0.02$, with 0.065 rms scatter. As the rms error expected observationally is less than the 7%, which is by far less than the error in other parameters (which are around 20%), we prefer not to add a new parameter in our analysis.

Here, $D_A(z_L, z_S)$ and $D_A(0, z_S)$ represent the angular diameter distance between lens and source and between observer and lens, respectively and z_L and z_S corresponds to the lens and source redshifts respectively. The ratio between these two angular diameter distances constraint cosmological models, since this distance in a flat FRW metric corresponds to

$$D_A(z, \mathbf{p}) = \frac{\overline{c}}{H_0(1+z)} \int_0^z \frac{dz'}{E(z'; \mathbf{p})}, \tag{2}$$

for a given z. The parameter $\mathbf{p}$ specifies the set of cosmological parameters that enter into the model, H_0 is the current value for the Hubble parameter. The function $E(z, \mathbf{p})$ represents the dimensionless expansion rate and it is obtained from the Friedmann Equation $H^2 \sim \rho$, where ρ represents the total energy density, via the ratio

$$E(z, \mathbf{p}) \equiv \frac{H(z, \mathbf{p})}{H_0}. \tag{3}$$

III. THE MODELS

In a flat FRW metric we consider the universe to be composed by pressureless matter, ρ_m, and an holographic dark energy component ρ_H. The Friedmann equation in this case

becomes

$$3H^2 = 8\pi\, G(\rho_m + \rho_H)\ . \tag{4}$$

Allowing the components to interact, we can write

$$\dot{\rho}_m + 3H\rho_m = Q = -\dot{\rho}_H - 3H(\rho_H + p_H). \tag{5}$$

where Q is an interaction term which can be an arbitrary function of the Hubble parameter H and the energy densities ρ_m and ρ_H, and p_H represents the pressure related to the holographic part. Here, the EoS parameter w is defined as the ratio p_H/ρ_H.

By introducing the ratio r between ρ_m and ρ_H so that $r = \rho_m/\rho_H$, we obtain the Hubble rate changes as

$$\frac{d\ln H}{d\ln a} = -\frac{3}{2}\left(1 + \frac{w(a)}{1+r(a)}\right)\ . \tag{6}$$

The parameter r changes as

$$\dot{r} = 3Hr\ (1+r)\ \left[\frac{w}{1+r} + \frac{Q}{3H\rho_m}\right]\ , \tag{7}$$

where equation (5) was used.

We may write the holographic energy density as [15, 18]

$$\rho_H = \frac{3\,c^2\,M_p^2}{L^2}\ , \tag{8}$$

where L represents the IR cutoff scale and M_p is the reduced Planck mass introduced previously (an arbitrary constant). In the holographic DE model it is assumed that the energy in a given box should not exceed the energy of a black hole of the same size. This means that

$$L^3\rho_H \leq M_p^2 L. \tag{9}$$

In this context the numerical constant c^2 is related with the degree of saturation of the previous expression.

Next we need to identify L with a cosmological length scale. In the literature, three choices of L have been considered: the Hubble scale, the future event horizon, and a scale proportional to the inverse square root of the Ricci scalar. Each of these cases will be analyzed in the subsequent sections.

Using (8) and (5) it is easy to see that

$$\Gamma \equiv \frac{Q}{\rho_H} = 2\frac{\dot{L}}{L} - 3H\left(1+w\right) \ , \tag{10}$$

where Γ corresponds to the rate by which ρ_H changes as a result of the interaction Q. In this expression, for $Q = 0$ there is a specific relationship between w and the ratio of the rates $\dot{L}/L$ and H. Of course, any non-vanishing Q will modify this relationship.

From expressions (10) and (7) it is found that the energy density ratio r evolves as

$$\dot{r} = -3H\ \left(1+r\right)\left[1 + \frac{w}{1+r} - \frac{2}{3}\frac{\dot{L}}{HL}\right] \ . \tag{11}$$

Note that, in general, different choices of the cutoff scale L result in different relations between w and r. It will turns out that for a Hubble-scale cutoff the ratio r is necessarily constant. For the other two choices, the future event horizon and the Ricci-scale cutoffs, the relationships between w and r vary with time. In particular, in both these cases a constant ratio r requires a constant EoS parameter w. In the following sections we study the three choices for L.

IV. RESULTS

In this section we perform the statistical analysis of each of the holographic models discussed in the previous section. The analytical derivation of each model was presented in [31] and here we only display a summary of the results.

In all the plots below, we explicitly show the 1σ and 2σ confidence contours, with (continues line) and without (dashed lines) the strong lensing data.

In order to probe the above models against observations, we consider four background tests which are directly related to the behavior of the function $H(z)$, i.e. the Hubble parameter as a function of the redshift z: SGL systems [27],[28],[29], supernova type Ia [34], massive and passively evolving early-type galaxies as "cosmic chronometers" [35], and other technics, which gives a direct measure of the $H(z)$ function [37], and the baryonic acoustic oscillations [5]. We shall present the results for a combined analysis of these four tests. Because all the models we consider, describe the universe evolution from the matter domination epoch to the onset of cosmic acceleration (where radiation is negligible) we only use the BAO data points from the WiggleZ experiment [38].

The supernova type Ia (SNIa) test is based on the luminosity distance function

$$D_L = (1+z)\frac{\overline{c}}{H_0}\int_0^z \frac{dz}{\sqrt{H(z)}}. \tag{12}$$

The observational relevant quantity is the moduli distance, given by

$$\mu = m - M = 5\ln\left(\frac{D_L}{Mpc}\right)+25, \tag{13}$$

where m is the apparent magnitude and M is the absolute magnitude of a given supernova. In what follows we shall use the data set of the Union2 sample [34].

The BAO measurements considered in our analysis are obtained from the WiggleZ experiment [38]. The χ^2 for the WiggleZ BAO data is given by

$$\chi^2_{WiggleZ} = (\bar{A}_{obs} - \bar{A}_{th})C^{-1}_{WiggleZ}(\bar{A}_{obs} - \bar{A}_{th})^T, \tag{14}$$

where the data vector is $\bar{A}_{obs} = (0.474, 0.442, 0.424)$ for the effective redshift $z = 0.44, 0.6$ and 0.73. The corresponding theoretical value $\bar{A}_{th}$ denotes the acoustic parameter $A(z)$ introduced by [5]:

$$A(z) = \frac{D_V(z)\sqrt{\Omega_m H_0^2}}{cz}, \tag{15}$$

and the distance scale D_V is defined as

$$D_V(z) = \frac{1}{H_0}\left[(1+z)^2 D_A(z)^2 \frac{cz}{E(z)}\right]^{1/3}, \tag{16}$$

where $D_A(z)$ is the Hubble-free angular diameter distance which relates to the Hubble-free luminosity distance through $D_A(z) = D_L(z)/(1+z)^2$. The inverse covariance $C^{-1}_{WiggleZ}$ is given by

$$C^{-1}_{WiggleZ} = \begin{pmatrix} 1040.3 & -807.5 & 336.8 \\ -807.5 & 3720.3 & -1551.9 \\ 336.8 & -1551.9 & 2914.9 \end{pmatrix}. \tag{17}$$

Another test we use is the age of the very old galaxies that have evolved passively. Our analysis is based on the 28 data points listed in reference [37]. The basic idea under this approach is based on the measurement of the differential age evolution as a function of redshift of these galaxies, which provides a direct estimate of the Hubble parameter $H(z) \simeq -1/(1+z)\triangle z/\triangle t$.

The fourth test comes from the formula of the Einstein radius for a singular isothermal sphere (SIS) model expressed by equation (1) which depends on the ratio of the angular

diameter distances between lens and source and between observer and lens. In this method, the cosmological information enters into a distance ratio

$$D^{th}(z_L, z_S) = \frac{\int_0^{z_S} dx/E(x)}{\int_{z_L}^{z_S} dx/E(x)}, \tag{18}$$

where the function E represents the dimensionless expansion rate introduced previously in (3). The observational data come from

$$D^{obs} = 4\pi \frac{\sigma_{SIS}^2}{\theta_E \, \overline{c}^2}. \tag{19}$$

For each of these observational tests we evaluate the fitting function χ^2, given by

$$\chi^2 = \sum_{i=1}^{n} \frac{(\epsilon_i^{th} - \epsilon_i^{ob})^2}{\sigma_i^2}, \tag{20}$$

where ϵ_i^{th} stands for a theoretical estimation of the ith data of a given quantity (moduli distance $\mu(z)$, parameters R and $\mathcal{A}$, $H(z)$), $D^{th}(z_L, z_S)$, and ϵ_i^{ob} stands for the corresponding observational data, σ_i being the error bar. In the following we will treat the cases separately.

A. Hubble radius

For $L = H^{-1}$ the holographic DE density is

$$\rho_H = 3\, c^2\, M_p^2\, H^2 \ . \tag{21}$$

a power of the Hubble rate, equivalent to

$$\frac{\Gamma}{3Hr} = \mu \left(\frac{H}{H_0}\right)^{-n} \tag{22}$$

The quantity μ is an interaction constant. Different interaction rates are characterized by different values of n. Considering $n \neq 0$ we found

$$H(z) = H_0 \left(\frac{1}{3}\right)^{1/n} \left[(1 - 2q_0) + 2(1 + q_0)(1 + z)^{\frac{3n}{2}}\right]^{\frac{1}{n}} . \tag{23}$$

The free parameters are H_0, q_0 and n. In a first step, the Hubble parameter H_0 is determined by minimizing the three-dimensional χ^2 function. The remaining parameters then are q_0 and n, for which we perform the statistical analysis. The results are displayed in Figure 1 As was mentioned in [31] this model for $n = 2$ is similar to the ΛCDM model.

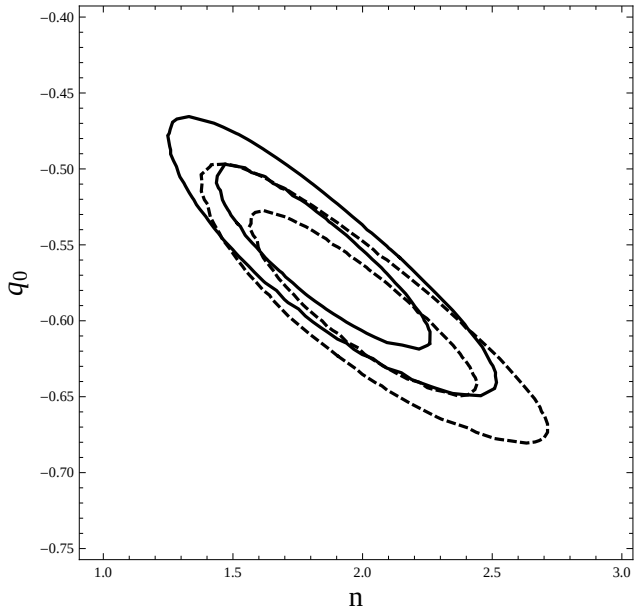


FIG. 1: Here we display the 68.27% and 95.45% confidence regions for the parameters q_0 and n of the Hubble-scale cutoff model of Eq.(23).

The best fit value for the parameters are $n = 1.82^{+0.44}_{-0.39}$ and $q_0 = -0.56^{+0.06}_{-0.06}$. The dark matter density used was $\Omega_m = 0.25$, and the best fitted value obtained for the Hubble parameter was $h = 0.697$. We use this value for h to obtain the confidence contour of the parameters displayed in Figure 1, showing that at one sigma this model is slightly different from the ΛCDM model. However, the $\chi^2_{red} = 1.213$ shows that this model is among the worst fit in this work although it is a reasonable fit, it is not as good as the ΛCDM model ($\chi^2_{red} = 1.030$). We also notice the impact of SGL data points. Considering they are only the 10% of the whole data set in this work, the SGL data shift the best fit to a smaller value for n and towards a slightly higher value for q_0.

B. Future event horizon with $\xi = 1$.

With $L = R_E$ the holographic DE density (8) is

$$\rho_H = \frac{3\,c^2\,M_p^2}{R_E^2}\ , \tag{24}$$

where

$$R_E(t) = a(t)\int_t^\infty \frac{dt'}{a(t')} = a\int_a^\infty \frac{da'}{H'\,a'^2} \tag{25}$$

is the future event horizon. The dark-energy balance (5) can be written as

$$\dot{\rho}_H + 3H(1 + w_{eff})\rho_H = 0 \tag{26}$$

with an effective EoS

$$w_{eff} = w + \frac{Q}{3H\rho_H} = -\frac{1}{3}\left(1 + \frac{2}{R_E H}\right) , \tag{27}$$

Although this quantity does not directly depend on w, the ratio r that enters $R_E H$ is determined by w via

$$\dot{r} = -H\,(1 + r)\left[1 + 3\frac{w}{1 + r} + \frac{2}{R_E H}\right] . \tag{28}$$

Assuming a power-law dependence for the energy-density ratio

$$r = r_0 a^{-\xi} . \tag{29}$$

we can solve the system. As was mentioned in [31] and [42], any value $\xi < 3$ makes the coincidence problem less severe than in the ΛCDM model. For this reason we consider the models with $\xi = 1, 2, 3$ separately. In the first case, $\xi = 1$ we obtain

$$H(z) = H_0(1 + z)^{3/2-1/c}\sqrt{\frac{1 + r_0(1 + z)}{r_0 + 1}}\left[\frac{\sqrt{r_0(1 + z) + 1} + 1}{\sqrt{r_0 + 1} + 1}\right]^{2/c} . \tag{30}$$

Since ξ is fixed, we have H_0, r_0 and c as free parameters. H_0 is obtained as in the previous case. The free-parameter space then consists of r_0 and c. The results are displayed in Figure 2.

The best fit value we obtained for the Hubble parameter was $h = 0.687$. Using it, the best fit parameters are $r_0 = 0.50^{+0.11}_{-0.09}$, and $c = 0.82^{+0.06}_{-0.06}$. The matter density is related to r_0 through $r_0 = \Omega_0/(1 - \Omega_0)$ then, our statistical analysis implies $\Omega_0 = 0.33^{+0.07}_{-0.06}$. The $\chi^2_{red} = 1.084$ indicates although it is a reasonable fit, being better than the Hubble Radius, it is not as good as the ΛCDM model ($\chi^2_{red} = 1.030$).

In comparison to the results of [31], our best fit values differs appreciably at one sigma, although at 3σ essentially there is no difference.

C. Future event horizon with $\xi = 2$.

Performing a similar analysis as before, this time with $\xi = 2$, we obtain

$$H(z) = H_0(1 + z)^{1-1/c}\sqrt{\frac{1 + r_0(1 + z)^2}{r_0 + 1}}\left[\frac{\sqrt{r_0(1 + z)^2 + 1} + 1}{\sqrt{r_0 + 1} + 1}\right]^{1/c} . \tag{31}$$

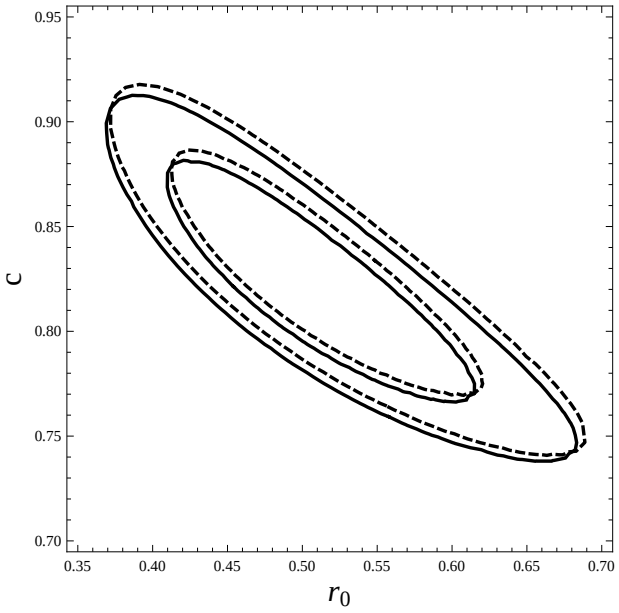


FIG. 2: Here we display the 68.27% and 95.45% confidence regions for the parameters r_0 and c of the Future event horizon model with $\xi = 1$ Eq.(30).

As in the previous case, the free parameters are H_0, r_0 and c. The results are displayed in Figure 3. The best fit we obtained for the Hubble parameter is $h = 0.697$. Using it, the best fit parameters are $r_0 = 0.43^{+0.09}_{-0.09}$, and $c = 1.02^{+0.11}_{-0.10}$. The matter density implied by our statistical analysis gives $\Omega_0 = 0.30^{+0.06}_{-0.05}$. The $\chi^2_{red} = 1.034$ shows this model is a competitive fit to all the data compared to the ΛCDM. In comparison to the results of [31], our best fit value for r_0 is essentially the same, although our best value for c is slightly higher at one sigma, at 3σ essentially there is no difference.

D. Future event horizon $\xi = 3$.

Using this time $\xi = 3$, we obtain:

$$H(z) = H_0(1+z)^{1/2-1/c}\sqrt{\frac{1+r_0(1+z)^3}{r_0+1}}\left[\frac{\sqrt{r_0(1+z)^3+1}+1}{\sqrt{r_0+1}+1}\right]^{2/(3c)} . \tag{32}$$

with confidence regions displayed in Fig.(4). The best fit value we obtained for the Hubble parameter is $h = 0.71$. The best fit parameters are $r_0 = 0.35^{+0.07}_{-0.06}$, and $c = 1.36^{+0.24}_{-0.20}$. The matter density implied by our statistical analysis gives $\Omega_0 = 0.26^{+0.05}_{-0.05}$. The $\chi^2_{red} = 1.052$ shows this among the best fit in this work. In comparison to the results of [31], our best fit

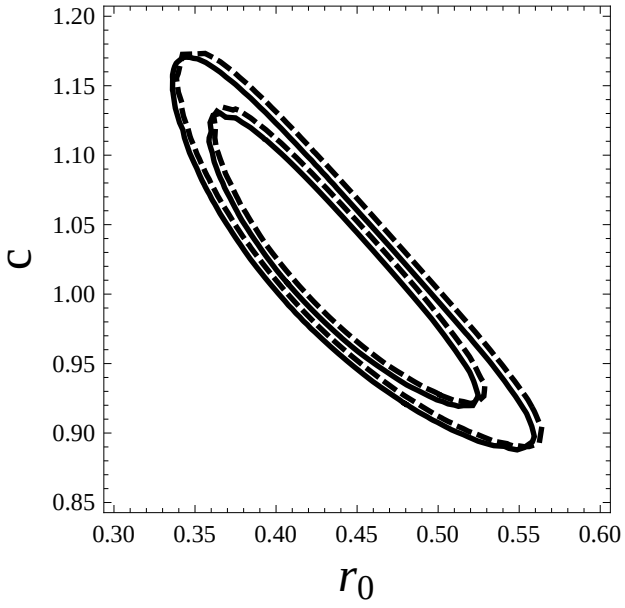


FIG. 3: Here we display the 68.27% and 95.45% confidence regions for the parameters r_0 and c of the Future event horizon model with $\xi = 2$ Eq.(31).

values differs completely even at 3σ.

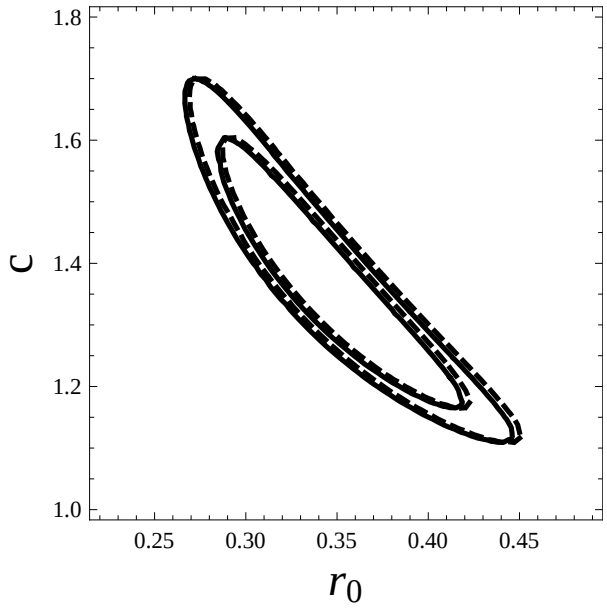


FIG. 4: Here we display the 68.27% and 95.45% confidence regions for the parameters r_0 and c of the Future event horizon model with $\xi = 3$ Eq.(32).

E. Ricci scale with CPL parametrization.

The Ricci scalar is given by $R = 6\left(2H^2 + \dot{H}\right)$. The corresponding cutoff-scale quantity is $L^2 = 6/R$, then

$$\rho_H = 3\,c^2\,M_p^2\,\frac{R}{6} = \alpha\left(2H^2 + \dot{H}\right)\ , \tag{33}$$

where $\alpha = \frac{3c^2}{8\pi G}$. As in the previous subsection, the balance equation (5) can be written as $\dot{\rho}_H + 3H\,(1 + w_{eff})\,\rho_H = 0$ where

$$w_{eff} = \frac{1}{1+r}\left(w + \frac{\dot{w}}{H}\right) = \frac{w + \frac{\dot{w}}{H}}{1 + r_0 + 3\,(w - w_0)}\ . \tag{34}$$

Here $r_0 = \frac{\Omega_{m0}}{1-\Omega_{m0}}$. The total effective EoS parameter is then given by

$$\frac{d\ln H}{d\ln a} = -\frac{3}{2}\frac{1 + r_0 + 4\left(w - \frac{3}{4}w_0\right)}{1 + r_0 + 3\,(w - w_0)}\ , \tag{35}$$

which can be integrated assuming a form for $w(a)$. Using the CPL parametrization $w(a) = w_0 + (1-a)w_1$ we obtain

$$H(z) = H_0(1+z)^{\frac{3}{2}\frac{1+r_0+\omega_0+4\omega_1}{1+r_0+3\omega_1}}\left[\frac{1 + r_0 + 3\omega_1\frac{z}{1+z}}{1+r_0}\right]^{-\frac{1}{2}\frac{1+r_0-3\omega_0}{1+r_0+3\omega_1}}\ . \tag{36}$$

The free parameters of this model are H_0, r_0, w_0 and w_1. In this case, the minimum value of the four-dimensional χ^2-function is used to determine both H_0 and r_0. Then, a two-dimensional analysis is performed for w_0 and w_1. The results are displayed in Figure 5. The best fit value we obtained for the Hubble parameter is $h = 0.706$ and also $r_0 = 0.41$, which translate in a matter density $\Omega_0 = 0.29$. Using it, the best fit parameters are $w_0 = -1.27^{+0.12}_{-0.13}$, and $w_1 = 0.99^{+0.30}_{-0.26}$. The $\chi^2_{red} = 1.036$ indicates this model is among the best fit in this work. In comparison to the results of [31], our best fit values are essentially the same at 1σ.

F. Ricci scale with interaction $Q = 3H\beta\rho_H$.

From the ansatz (33), in general we can write a relation for the interaction term

$$Q = -\frac{3H}{1+r}\left[rw - \frac{\dot{w}}{H}\right]\rho_H\ . \tag{37}$$

which is a property of the model. Combining this with $Q = 3H\beta\rho_H$, we can get a first-order differential equation for w which has the solution

$$w = -\frac{1}{6}\frac{u - s - (u+s)\ A\,a^s}{1 - A\,a^s}\ , \tag{38}$$

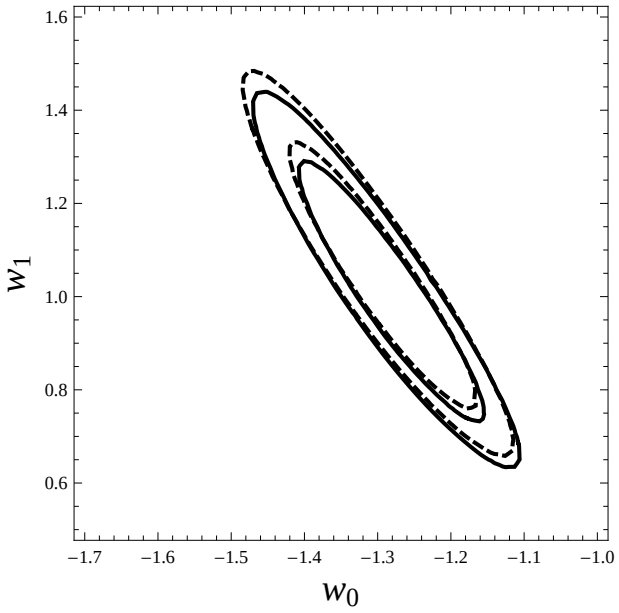


FIG. 5: Here we display the 68.27% and 95.45% confidence regions for the parameters w_0 and w_1 of the Hubble-scale cutoff model of Eq.(36).

where

$$u \equiv r_0 - 3w_0 + 3\beta \ , \qquad v \equiv r_0 + 3w_0 + 3\beta \ , \quad s \equiv \sqrt{u^2 - 12\beta\,(1 + r_0 - 3w_0)} \tag{39}$$

and

$$A \equiv \frac{v - s}{v + s} \ . \tag{40}$$

Using this form (38) for $w(a)$ we obtain

$$H(z) = H_0(1+z)^{\frac{3}{2}\left(1-\frac{k}{m}\right)} \left\{ \frac{n(1+z)^{-s} - m}{n - m} \right\}^{\frac{3}{2}\frac{lm-kn}{mns}} \ . \tag{41}$$

Here, one has H_0, r_0, w and β as free parameters. We fix $w = -1$ and determine H_0 along the lines already described for the previous cases. The results are displayed in Fig.(6). The best fit value we obtained for the Hubble parameter was $h = 0.70$, assuming the value $w = -1$. The best fit parameters are $r_0 = 0.39^{+0.06}_{-0.06}$, and $\beta = 0.10^{+0.06}_{-0.06}$. The $\chi^2_{red} = 1.033$ shows this model is one of the best fit in this work, with a negligible statistical difference with respect to the ΛCDM (See Table I). In comparison to the results of [31], our best fit values are essentially the same at 1σ.

As a summary of our results we display the χ^2_{min}, and the Akaike Information Criteria (AIC) and Bayesian Information Criteria (BIC) for each model, in comparison with the

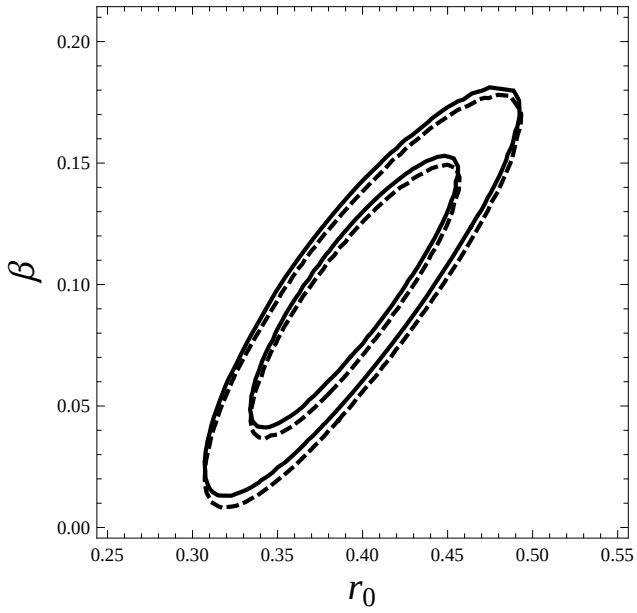


FIG. 6: Here we display the 68.27% and 95.45% confidence regions for the parameters r_0 and β in the Ricci scale with interaction model of Eq.(41).

ΛCDM model in Table I. Although the ΛCDM model is the best fit to the data, considering the χ^2_{min} values, the Future Event Horizon model with $\xi = 2$ and both Ricci scale models (with CPL and interaction), appears in reasonable statistical agreement with the data. However, considering the number of free parameters of each model, using for example the BIC criteria [79], neither of these models are really competitive with the ΛCDM model.

V. CONCLUSION

In this work we have used strongly gravitationally lensed (SGL) systems, to provide additional constraints on a set of holographic dark energy models previously considered in [31]. In addition to the SGL data, in this paper we have used the largest set of measurements of the Hubble parameter $H(z)$ in the range of redshifts $0.07 \leq z \leq 2.3$ [37], recent data from BAO [38] and supernovae [34].

We found that the ΛCDM, with two free parameters Ω_m and h, is the best fit to all the data. Although the statistical comparison among χ^2_{min} values seems to indicate that the Future Event Horizon with $\xi = 2$, and the Ricci scale holographic model, show interesting agreement with the observations, using a stringent test, using the AIC and BIC criteria, lead

	ΛCDM	Hubble Radius	Future ($\xi = 1$)	Future ($\xi = 2$)	Future ($\xi = 3$)	Ricci CPL	Ricci with Q
χ^2_{min}	675.57	794.37	710.01	677.14	689.34	677.51	675.28
χ^2_{red}	1.030	1.213	1.084	1.034	1.052	1.036	1.033
$\triangle$AIC	0	121	36	3.6	16	3.9	3.7
$\triangle$BIC	0	125	41	8.1	20	15	13

TABLE I: This table is a summary of the statistical analysis using all the data; 557 SNIa, 70 Strong Lensing points, 28 Hubble function points, and three BAO scale points. We show both the χ^2_{min} and the reduced χ^2_{red}, which takes into account the number of free parameters to fit the data. We observe that, although the χ^2_{min} values for the Future Event Horizon with $\xi = 2$, and the Ricci scale with interaction model, show a fit similar to the ΛCDM, taking into account the number of free parameters for each model, through the AIC and BIC criteria, the data suggest neither of the holographic models is competitive with the ΛCDM model.

us to the result that neither of the holographic models are competitive with the ΛCDM.

These results show the importance of Strong Lensing measurements to provide additional observational constraints to alternative cosmological models, which are necessary to shed some light into the dark universe.

Acknowledgments

This work was funded by Comision Nacional de Ciencias y Tecnología through FONDECYT Grants 1110230 (SdC and VHC), 1120741 (AB,VM), and also from DI-PUCV Grants 123.710 (SdC) and through DIUV grant 13/2009 (VHC).

[1] A. G. Riess et al., Astron. J. 116, 1009 (1998)[astro-ph/9805201]; S. J. Perlmutter et al., Astrophys. J. 517, 565(1999); A. G. Riess et al., Astrophys. J. 607, 665(2004); P. Astier et al., Astron. Astrophys. 447, 31 (2006).

[2] M. Tegmark et al. [SDSS Collaboration], Phys. Rev. D 69, 103501 (2004); K. Abazajian et al. [SDSS Collaboration], Astron. J. 128, 502 (2004); K. Abazajian et al. [SDSS Collaboration],

Astron. J. 129, 1755 (2005).

[3] H. V. Peiris et al., Astrophys. J. Suppl. 148 (2003) 213 [astro-ph/0302225]; C. L. Bennett et al., Astrophys. J. Suppl. 148 1 (2003); D. N. Spergel et al., Astrophys. J. Suppl. 148 175 (2003).

[4] S. Boughn and R. Chrittenden, Nature (London) **427**, 45 (2004); P. Vielva, E. Martínez–González, and M. Tucci, Mon. Not. R. Astron. Soc. **365**, 891 (2006).

[5] D. J. Eisenstein *et al.* [SDSS Collaboration], Astrophys. J. **633**, 560 (2005) [astro-ph/0501171].

[6] C.R. Contaldi, H. Hoekstra, and A. Lewis, Phys. Rev. Lett. **90**, 221303 (2003).

[7] S. Weinberg, Rev. Mod. Phys. 61, 1 (1989); E.J. Copeland, M. Sami, S. Tsujikawa, Int. J. Mod. Phys. D 15, 1753 (2006).

[8] C. Wetterich, Nucl. Phys. B 302, 668 (1988); B. Ratra, J. Peebles, Phys. Rev. D 37, 321 (1988).

[9] T. Chiba, T. Okabe, M. Yamaguchi, Phys. Rev. D 62, 023511 (2000); C. Armendariz-Picon, V. Mukhanov, P.J. Steinhardt, Phys. Rev. Lett. 85, 4438 (2000).

[10] A. Sen, J. High Energy Phys. 10, 008 (1999); E.A. Bergshoeff, M. de Roo, T.C. de Wit, E. Eyras, S. Panda, J. High Energy Phys. 05, 009 (2000).

[11] C. Wetterich, Nucl. Phys. B **302**, 668 (1988); *ibid.* Astron. Astrophys. **301**, 321 (1995).

[12] A. Kamenshchik, U. Moschella, V. Pasquier, Phys. Lett. B 511, 265 (2001).

[13] W.S. Hipólito-Ricaldi, H.E.S. Velten and W. Zimdahl, Phys. Rev. D **82**, 063507 (2010).

[14] P. Horava, D.Minic, Phys. Rev. Lett. 85, 1610 (2000); S. Thomas, Phys. Rev. Lett. 89, 081301 (2002).

[15] A. G. Cohen, D.B. Kaplan and A.E. Nelson, Phys. Rev. Lett. **82**, 4971 (1999).

[16] G. t Hooft, gr-qc/9310026; L. Susskind, J. Math. Phys. 36, 6377 (1995)

[17] W. Fischler and L. Susskind, arXiv:hep-th/9806039 (1998).

[18] M. Li, Phys. Lett. B **603**, 1 (2004).

[19] C. Gao, F. Q. Wu, X. Chen and Y. G. Shen, Phys. Rev. D **79**, 043511 (2009).

[20] C. J. Feng, Phys. Lett. B **670**, 231 (2008); L. N. Granda and A. Oliveros, Phys. Lett. B **669**, 275 (2008).

[21] X. Zhang and F. Q. Wu, Phys. Rev. D 72, 043524 (2005) ; Z. Chang, F. Q. Wu and X. Zhang, Phys. Lett. B **633**, 14 (2006); K. Enqvist, S. Hannestad and M. S. Sloth, JCAP **0502** 004 (2005); J. Shen, B. Wang, E. Abdalla and R. K. Su, Phys. Lett. B **609**, 200 (2005).

[22] Q. G. Huang and M. Li, JCAP 0408, 013 (2004).

[23] B. Wang, Y.G. Gong and E. Abdalla, Phys. Lett. B **624**, 141 (2005).

[24] F.C. Carvalho and A. Saa, Phys. Rev. D70, 087302 (2004); L. Perivolaropoulos, JCAP **0510**, 001 (2005).

[25] Y.G. Gong, Phys. Rev. D **70**, 064029 (2004);

[26] W. Zimdahl and D. Pavón, Class. Quantum Grav. **24**, 5641 (2007); W. Zimdahl, IJMPD **17**, 651 (2008).

[27] T. Futamase and S. Yoshida, Prog. Theor. Phys. **105**, 887 (2001).

[28] M. Biesiada, Phys. Rev. D **73**, 023006 (2006).

[29] S. Cao, Y. Pan, M. Biesiada, W. Godlowski and Z. -H. Zhu, JCAP **1203**, 016 (2012) [arXiv:1105.6226 [astro-ph.CO]].

[30] K. Liao and Z. -H. Zhu, Phys. Lett. B **714**, 1 (2012) [arXiv:1207.2552 [astro-ph.CO]].

[31] S. del Campo, J. .C. Fabris, R. Herrera and W. Zimdahl, Phys. Rev. D **83**, 123006 (2011) [arXiv:1103.3441 [astro-ph.CO]].

[32] D. Walsh, R.F. Carswell and R.J. Weymann, Nature, **279**, 381 (1979).

[33] A comprehensive review of the theory see P. Schneider, J. Ehlers, & E. Falco *Gravitational lensing*, Springer-Verlag, Berlin (1992), and M. Bartelmann, Classical and Quantum Gravity, **27**, 233001 (2010). See also C.S. Kochanek, *Gravitational Lensing: Strong, Weak and Micro*, Saas-Fee Advanced Course **33**, Springer, Berlin (2006).

[34] R. Amanullah *et al.*, Astrophys. J. **716**, 712 (2010) [arXiv:1004.1711 [astro-ph.CO]].

[35] R. Jimenez and A. Loeb, Astrophys. J. **573**, 37 (2002) [astro-ph/0106145].

[36] M. Moresco, A. Cimatti, R. Jimenez, L. Pozzetti, G. Zamorani, M. Bolzonella, J. Dunlop and F. Lamareille *et al.*, JCAP **1208**, 006 (2012) [arXiv:1201.3609 [astro-ph.CO]].

[37] O. Farooq and B. Ratra, Astrophys. J. **766**, L7 (2013) [arXiv:1301.5243 [astro-ph.CO]].

[38] C. Blake, E. Kazin, F. Beutler, T. Davis, D. Parkinson, S. Brough, M. Colless and C. Contreras *et al.*, Mon. Not. Roy. Astron. Soc. **418**, 1707 (2011) [arXiv:1108.2635 [astro-ph.CO]].

[39] J.R. Bond, G. Efstathiou e M. Tegmark, Month. Not. R. Astron. Soc. **291**, L33(1997).

[40] E. Komatsu et al., Astrophys. J. Suppl. **192**, 18(2011).

[41] M. Moresco, L. Verde, L. Pozzetti, R. Jimenez and A. Cimatti, JCAP **1207**, 053 (2012) [arXiv:1201.6658 [astro-ph.CO]].

[42] N. Dalal, K. Abazajian, E. Jenkins, and A.V. Manohar, Phys. Rev. Lett. **86**, 1939 (2001).

[43] L.V. Koopmans and T. Treu, Astrophys. J. **568**, L5 (2002)

[44] L.V. Koopmans & T. Treu, Astrophys. J. **583**, 606 (2003)

[45] L.V. Koopmans, T. Treu, A.S. Bolton, S. Burles, L.A. Moustakas, Astrophys. J. **649**, 599 (2006)

[46] L.V. Koopmans, A.S. Bolton, T. Treu, O. Czoske, M.W. Auger, M. Bernabe, S. Vegetti, R. Gavazzi, L.A. Moustakas, S. Burles Astrophys. J. **703**, L51 (2009)

[47] T. Treu, L.V. Koopmans, A.S. Bolton, S. Burles, L.A. Moustakas, Astrophys. J. **640**, 662 (2006)

[48] T. Treu, L.V. Koopmans, A.S. Bolton, S. Burles, L.A. Moustakas, Astrophys. J. **650**, 1219 (2006)

[49] C. Grillo, M. Lombardi, P. Rosati, G. Bertin, R. Gobat, R. Demarco, C. Lidman and V. Motta *et al.*, arXiv:0805.2381 [astro-ph].

[50] R.C. Bolton, S. Burles, D.J. Schlegel, D.J. Eisenstein, J. Brinkmann, Astron. J. **127**, 1860 (2004)

[51] R.C. Bolton, S. Burles, L.V. Koopmans, T. Treu, R. Gavazzi, L.A. Moustakas, R. Wayth, D.J. Schlegel, Astrophys. J. **682**, 964 (2008)

[52] M.W. Auger, T. Treu, A.S. Bolton, R. Gavazzi, L.V.E. Koopmans, P. Marshall, K. Bundy, L.A. Moustakas, Astrophys. J. **705**, 1099 (2009)

[53] N. Ota & K. Mitsuda, Astron. Astrophys. **428**, 757 (2004)

[54] H. Yu and Z. -H. Zhu, Res. Astron. Astrophys. **11**, 776 (2011) [arXiv:1011.6060 [astro-ph.CO]].

[55] S. Refsdal, Mon. Not. R. Astron. Soc. **132**, 101 (1966)

[56] R.D. Blandford, R. Narayan, Astron. Astrophys. **30**, 311 (1992)

[57] E.L. Turner, Astrophys. J. **365**, L43 (1990).

[58] M. Fukugita, T. Futamase and M. Kasai, Mon. Not. Roy. Astron. Soc. **246**, 24P (1990).

[59] K. -H. Chae, Mon. Not. Roy. Astron. Soc. **346**, 746 (2003) [astro-ph/0211244].

[60] J. L. Mitchell, C. R. Keeton, J. A. Frieman and R. K. Sheth, Astrophys. J. **622**, 81 (2005) [astro-ph/0401138].

[61] M. Oguri, N. Inada, J. A. Blackburne, M. -S. Shin, I. Kayo, M. A. Strauss, D. P. Schneider and D. G. York, Mon. Not. Roy. Astron. Soc. **391**, 1973 (2008) [arXiv:0809.0913 [astro-ph]].

[62] C.S. Kochanek, Astrophys. J. **397**, 381 (1992).

[63] E. O. Ofek, H. -W. Rix and D. Maoz, Mon. Not. Roy. Astron. Soc. **343**, 639 (2003)

[astro-ph/0305201].

[64] K. -H. Chae and S. Mao, Astrophys. J. **599**, L61 (2003) [astro-ph/0311203].

[65] A. Matsumoto and T. Futamase, Mon. Not. Roy. Astron. Soc. **384**, 843 (2008) [arXiv:0712.0215 [astro-ph]].

[66] K. -H. Chae, arXiv:0811.0560 [astro-ph].

[67] S. Cao and Z. -H. Zhu, Astron. Astrophys. **538**, A43 (2012) [arXiv:1105.6182 [astro-ph.CO]].

[68] A.G. Riess, W.H. Press and R.P. Kirshner, Astrophys. J. **473**, 588 (1996).

[69] S. Eales, L. Dunne, D. Clements et al., 2010 PASP, 122, 499.

[70] Y. D. Hezaveh, D. P. Marrone, C. D. Fassnacht, J. S. Spilker, J. D. Vieira, J. E. Aguirre, K. A. Aird and M. Aravena *et al.*, Astrophys. J. **767**, 132 (2013) [arXiv:1303.2722 [astro-ph.CO]].

[71] T. Treu, P. J. Marshall, F. Y. Cyr-Racine, C. D. Fassnacht, C. R. Keeton, E. V. Linder, L. A. Moustakas and M. Bradac *et al.*, arXiv:1306.1272 [astro-ph.CO].

[72] C.S. Kochanek, E.E. Falco, C. Impey, J. Lehar, B. McLeod, H.-W. Rix, *www.cfa.harvard.educastles*

[73] C.S. Kochanek, Astrophys. J. **473**, 595 (1996)

[74] D. Rusin & C.S. Kochanek, Astrophys. J. **623**, 666 (2005)

[75] F.D. Fassnacht & J.G. Cohen, Astrophys. J. **115**, 377 (1998)

[76] L.J. King, I.W.A. Browne, T.W.B. Muxlow, D. Narasimha, A.R. Patnaik, R.W. Porcas, P.N. Wilkinson, Mon. Not. R. Astron. Soc. **289**, 450 (1997).

[77] E. White and D. S. Davis, Bull. Am. Astron. Soc. **28**, 1323 (1998).

[78] N. Wang and L. Xu, Modern Physics Letters A Vol. 28, No. **14**, 1350057 (2013) [arXiv:1309.0887 [astro-ph.CO]].

[79] R. Kass and A. Raftery, J. Am. Statist. Assoc. **90**, 773-795 (1995).